

Identification of Numerically Accurate First-Order
Takagi-Sugeno Systems with Interpretable Local Models
From Data

Andri Riid and Ennu Rüstern

Department of Computer Control

Tallinn University of Technology

Ehitajate tee 5, Tallinn, 19086, Estonia

Abstract - The paper deals with the interpretability problem of 1st order Takagi-Sugeno systems and interpolation issues in particular. Interpolation improvement is carried out by a corrective secondary model (essentially a black box) complementing the primary (interpretable) model. Optimization technique for this two-model configuration is developed. Experimental results suggest that this approach achieves a better accuracy-interpretability tradeoff than the methodologies currently in use.

Keywords:

Fuzzy systems, inference mechanism, modeling, interpolation.

1. Introduction

The fuzzy inference system introduced by Takagi and Sugeno (1st order TS system) in (1) is a powerful tool for modeling complex nonlinear systems. TS modeling is a multimodel approach in which linear local models associated with TS rules are combined to describe the global behavior of the system. TS rules have high degrees of freedom to improve their performance that makes it possible to express complicated behaviors with a small number of rules which, in consequence, has made 1st order TS system overwhelmingly popular in the applications of fuzzy logic.

The local models of a TS system are expected to admit valid interpretation as local linearizations of the modeled nonlinear system, allowing one to gain insight into the behavior of the system (interpretation in terms of linearizations is useful in system analysis and local control design, for example in gain-scheduled control (2)). Most applications of fuzzy logic, however, ignore the linguistic aspect of 1st order TS systems and use them as a substitute of neural networks. Admittedly, it is difficult to obtain interpretable as well as accurate TS systems because of the trade-off between these requirements in fuzzy logic systems (3) that can be quite drastic (4).

This paper's goal is to focus on this problem. Interpretability problem can be contributed to overparameterization as much as to undesirable properties of TS rule interpolation mechanism. In section 3, it is demonstrated that existing interpretability improvement techniques (5,6) deal primarily with overparameterization and the expected solution has to consider the interpolational aspect, as well. For this purpose, we introduce a two-model system configuration (section 4), which includes an additional secondary model complementing the primary (interpretable) one to cancel out the undesired effects of TS inference. To use this approach in practice, an optimization method is developed (section 5). The modeling experiments with the

aforementioned system configuration and optimization method presented in section 6 demonstrate that it is possible obtain accurate and interpretable models within TS modeling paradigm.

2. Takagi-Sugeno systems

We consider multi-input/single-input first-order TS fuzzy systems consisting of R rules (1), where A_{ir} denote the linguistic labels of the i^{th} input variable ($i = 1 \dots N$), associated with the r^{th} rule, having one-to-one correspondence with normal and convex MFs μ_{ir} in the inference function (2) (where τ_r denotes the activation degree of the r^{th} rule); p_{0r}, p_{ir} denote the consequent parameters of the r^{th} rule, x_i denotes the numerical value of the i^{th} input variable and τ_r is the activation degree of the r^{th} rule.

$$\begin{aligned} &\text{IF } x_1 \text{ is } A_{1r} \text{ AND } \dots \text{AND } x_i \text{ is } A_{ir} \text{ AND } \dots \text{AND} \\ &x_N \text{ is } A_{Nr} \text{ THEN } y_r = p_{0r} + \dots + p_{ir}x_1 + \dots p_{Nr}x_N, \end{aligned} \quad (1)$$

$$y = \frac{\sum_{r=1}^R y_r \prod_{i=1}^N \mu_{ir}(x_i)}{\sum_{r=1}^R \prod_{i=1}^N \mu_{ir}(x_i)} = \frac{\sum_{r=1}^R \tau_r y_r}{\sum_{r=1}^R \tau_r}. \quad (2)$$

With the given system configuration, our natural expectation is that the global output y of the system is formed of distinct and smoothly interpolated local models y_r as depicted in Fig. 1.

Figure 1

This expectation, however, is bound to fail because overparameterization that makes 1st order TS systems so effective in modeling, results in nonuniqueness in model structure by what different parameter vectors may yield the same input/output behavior. Moreover, large perturbations of consequent parameters may have a very small effect on global approximation. This is illustrated in Fig. 2., where 4 four three-

rule TS models approximate a simple function. Overparameterization of 1st order TS systems is further emphasized by the fact that all these fuzzy approximations share the same input partition (consisting of 3 triangular MFs, centered at $x = 0.3, 0.95,$ and 1.6).

Figure 2

Obviously, this situation commands for the appropriate measure of interpretability. E.g. given K pairs of input-output data $[\mathbf{x}(k) \ y(k)]$, the interpretation error can be computed by

$$\varepsilon_l = \sqrt{\frac{\sum_{r=1}^R \sum_{k=1}^K \tau_r(k) (y(k) - y_r(k))^2}{KR}}, \quad (3)$$

which is a weighted (by τ_r) average of the difference between the global output y and all local models y_r . For the systems depicted in Fig. 2, the corresponding values of ε_l are 1.3139, 0.1306, 0.0313, and 1.2922; clearly indicating which system is the best from interpretational viewpoint.

Interpretability of a 1st TS system depends on how the optimization method applied uses its free parameters. Typically, the system parameters in TS optimization are obtained by global learning strategies that concentrate on minimizing quadratic global cost function, paying little attention to interpretability. For example, on the assumption that the rulebase and input MFs of the model are defined (extracted from expert knowledge, using a clustering method ^(7,8) or yet some other technique), consequent parameters of TS systems are almost exclusively identified by a (global) least squares estimator ⁽¹⁾. Using the notations $X_e = [1 \ \mathbf{X}]$ with rows $[1 \ \mathbf{x}_k]$, $\mathbf{x}_k = [x_1(k), x_2(k), \dots, x_N(k)]$ and $\Gamma = [W_1 X_e, W_2 X_e, \dots, W_r X_e, \dots, W_R X_e]$, where

$$W_r = \begin{bmatrix} \beta_r(1) & 0 & \dots & 0 \\ 0 & \beta_r(2) & \dots & 0 \\ \dots & \dots & \dots & \dots \\ \dots & \dots & \dots & \beta_r(K) \end{bmatrix}, \quad (4)$$

and where $\beta_r(k) = \tau_r(k) / \sum_{r=1}^R \tau_r(k)$ (normalized rule activation degree), (2) becomes

equivalent to a least squares problem $y = \Gamma\theta + \varepsilon$, where ε is the approximation error, which has the solution, given by (5)

$$\theta = [\Gamma^T \Gamma]^{-1} \Gamma^T y, \quad (5)$$

where $\theta = [p_1, \dots, p_r, \dots, p_R]^T$, $p_r = [p_{0r}, p_{1r}, \dots, p_{ir}, \dots, p_{Nr}]$.

3. Overview of existing interpretability improvement schemes

To improve interpretability of the local models and consequently interpretability of the global model, there are principally two possibilities. First is to replace global LSE with the local (or weighted) version ⁽⁹⁾ that estimates the parameters of the local models separately.

$$\theta_r = [X_e^T W_r X_e]^{-1} X_e^T W_r y, \quad r = 1 \dots R, \quad (6)$$

W_r has nonzero values only in a limited region of input space that explains why each extracted fuzzy rule acts like an independent model related to a subset of training data that is encouraged to produce the whole of the output rather than a component of it. It

is also possible to calculate θ in one compact least squares problem

$$\theta = [\bar{X}_e^T \bar{W} \bar{X}_e]^{-1} \bar{X}_e^T \bar{W} \bar{y}, \quad (7)$$

$$\text{where } \bar{y} = [y, y, \dots, y]^T, \quad \bar{X}_e = \begin{bmatrix} X_e & 0 & \dots & 0 \\ 0 & X_e & \dots & 0 \\ \dots & \dots & \dots & \dots \\ \dots & \dots & \dots & X_e \end{bmatrix}, \quad \bar{W} = \begin{bmatrix} W_e & 0 & \dots & 0 \\ 0 & W_e & \dots & 0 \\ \dots & \dots & \dots & \dots \\ \dots & \dots & \dots & W_e \end{bmatrix}.$$

However, weighted parameter estimation gives an optimal estimate of the local models and does not provide an optimal fuzzy model in terms of minimal modeling error because the aggregation of the rules is not taken into account. That problem is handled by a combined local-global LSE approach proposed in ⁽⁵⁾ that aims at striking a good tradeoff between the global approximation and local interpretation, determined by positive constants λ_1 and λ_2 ($\lambda_1 + \lambda_2 = 1$) in (8).

$$\theta = (\lambda_1 \Gamma^T \Gamma + \lambda_2 \bar{X}_e^T \bar{W} \bar{X}_e)^{-1} (\lambda_1 \Gamma^T y + \lambda_2 \bar{X}_e^T \bar{W} \bar{y}) \quad (8)$$

The alternative way for interpretability improvement can be derived from the expression of interpretability error (3). Apparently, ε_l can be minimized by reducing the role of rule interpolation in the model so that for each given data pair one rule dominates over the other rules (has significantly higher value of τ_r). This can be accomplished e.g. by controlling the overlap of adjacent input MFs ⁽¹⁰⁾. ε_l could even be reduced to zero by using boxlike MFs but it has two co-effects. First, technically, such system is a classical logic based system than a fuzzy system. Secondly, isolation of rules hampers system adaptability. Finding the optimal interpolation/isolation balance is therefore not a trivial task. Perhaps the most effective implementation of this strategy is to exponent rule fulfillment degrees directly in the input space as suggested in ⁽⁶⁾ so that in (4)

$$\beta_r(k) = (\tau_r(k))^m / \sum_{r=1}^R (\tau_r(k))^m, \quad (9)$$

where $m > 1$ is the rule exponent. When applying global LSE (5), the higher value of m leads to improved interpretability.

The following example demonstrates the effect of described techniques on the identification of a simple single-input function

$$y = 0.7 \sin(1.1x) + 0.3 \cos(2.2x) - \cos(0.4x) \quad (10)$$

Figure 3

Training data set consists of 113 uniformly distributed samples in $x = [-2.1, 3.6]$. Four local models are used, input partition consists of five triangular MFs, centered at the points where the second derivative of (10) is equal to zero (Fig. 3). Application of global LSE, weighted LSE ($\lambda_1 = 0.9, \lambda_2 = 0.1$) and global LSE with exponented rules ($m = 2$) results in three models depicted in Fig. 5. Modeling and interpretability errors are given in Table 1.

Figure 4

Figure 5

As we see, both these techniques are able to extract the local models with considerably more local context the problem can be reduced to a certain level only because of the interpolation properties of the TS inference mechanism, which are observed in greater detail in the following simple example.

Table 1

Tradeoff between interpretability and accuracy becomes very evident here. First, interpolated global output from two neighboring interpretable local models is quite different from the one that one would be expecting intuitively (Fig. 6). On the other hand, in order to produce the desired smooth interpolated output with (2), we need to sacrifice interpretability – two interpolating local models give substantially biased local linear estimates of the inferred global function. (Fig 7).

Figure 6

Figure 7

There is no straightforward solution¹ to this problem except a certain compromise – we insert an additional rule (see Fig. 8) that on one hand would improve interpolation

¹ For example, the issue has been investigated in (¹¹) where the authors propose to replace TS inference mechanism with a smoothing maximum functional, which only arises further problems.

between two existing interpretable rules but on the other hand, interpretability of the inserted rule must be sacrificed. The latter deficiency, however, is acceptable if information about interpretability of any given rule is known (non-transparency can be localized). We accomplish that by organizing interpretable and interpolating rules into separate models as shown in the next section.

Figure 8

4. System Configuration

To distinguish between interpretable and interpolating rules they are divided between two submodels – primary (interpretable) and secondary (interpolative). Each MF μ_i^s ($i = 1 \dots N$, $s = 1 \dots S_i$ ($S_i > 1$)) of the i^{th} input variable of the primary model is defined by a set of four parameters – a_i^s, b_i^s, c_i^s and d_i^s – and the underlying spline-based function (11).

$$\mu_i^s(x_i) = \begin{cases} 0, & \text{if } x_i < a_i^s \text{ or } x_i < d_i^s \\ 2 \left(\frac{x_i - a_i^s}{b_i^s - a_i^s} \right)^2, & \text{if } a_i^s \leq x_i \leq \frac{a_i^s + b_i^s}{2} \\ 1 - 2 \left(\frac{b_i^s - x_i}{b_i^s - a_i^s} \right)^2, & \frac{a_i^s + b_i^s}{2} \leq x_i \leq b_i^s \\ 1, & \text{if } b_i^s < x_i \leq c_i^s \\ 1 - 2 \left(\frac{x_i - c_i^s}{d_i^s - c_i^s} \right)^2, & \text{if } c_i^s \leq x_i \leq \frac{c_i^s + d_i^s}{2} \\ 2 \left(\frac{d_i^s - x_i}{d_i^s - c_i^s} \right)^2, & \frac{c_i^s + d_i^s}{2} \leq x_i \leq d_i^s \end{cases} \quad (11)$$

Note that the following constraints apply:

$$\mu_i^s : a_i^s = c_i^{s-1}, d_i^s = b_i^{s+1}, \quad (12)$$

except when $s = 1$: $a_i^s = b_i^s$ and when $s = S_i$ $d_i^s = c_i^s$ (Fig. 9).

MFs γ_i^t ($t = 1, \dots, T_i$ ($T_i = 2S_i - 1$)) of the secondary model use the same

underlying function, (to avoid the confusion, its four parameters are denoted by $\alpha_i^t, \beta_i^t, \chi_i^t$ and δ_i^t) and their parameters are derived directly from the input partition of the primary model (Fig. 10).

$$\gamma_i^t \equiv \mu_i^s, \text{ if } t=2s-1 \text{ (} s=1, \dots, S_i \text{)}.$$

$$\gamma_i^t : \alpha_i^t = c_i^s, \delta_i^t = d_i^s, \beta_i^t = \chi_i^t = \frac{c_i^s + d_i^s}{2}, \text{ if } t=2s \text{ (} s=1, \dots, S_i-1 \text{)}. \quad (13)$$

Note that trapezoid type of membership function can be used instead of (11), with (12-13) remaining valid.

Figure 9

Figure 10

Primary model has fully defined combinatorial rulebase (which means that all possible combinations of input MFs are described by it, bringing the total number of rules to $P = \prod_{i=1}^N S_i$). From the rulebase of the secondary model, initially obtained in the similar manner, however, the rules that satisfy (14) are excluded because they are already described by the primary model.

$$\forall i, (\chi_{ir} - \beta_{ir} > 0), r = 1, \dots, R, (R = \prod_{i=1}^N T_i), \quad (14)$$

where χ_{ir} and β_{ir} denote the parameters of the MF of the i^{th} input variable associated with the r^{th} initial rule. After rule filtering we should have $Q = R - P$ rules in the secondary model.

Global output of the whole system is computed by

$$y = y_1 + y_2 = \sum_{p=1}^P y_p \tau_p \left/ \sum_{q=1}^Q \tau_q \right. + \sum_{q=1}^Q y_q \tau_q \left/ \sum_{q=1}^Q \tau_q \right. \quad (15)$$

Note that the type of the consequent function y_q of the secondary model does not necessarily need to be a 1st order function as in the primary model. In some cases

higher order consequent functions can be more effective because of their extended interpolative power, or on the other hand, sometimes it may be just sufficient to use a constant consequent (0th order function). In particular, the following consequent function types (besides the constant ($y_q = p_{0q}$) and the original one given in (2)) have been considered in current paper:

$$y_q = p_{0q} + \sum_{i=1}^N p_{iq}^{(1)} x_i + \sum_{i=1}^N p_{iq}^{(2)} x_i^2, \quad (16)$$

$$y_q = p_{0q} + \sum_{i=1}^N p_{iq}^{(1)} x_i + \sum_{i=1}^N p_{iq}^{(2)} x_i^2 + \sum_{i=1}^N p_{iq}^{(3)} x_i^3, \quad (17)$$

5. Optimizing the System

The (supervised) optimization method described in this section requires a set of training data consisting of K training samples $[\mathbf{x}_k \ y(k)]$, predefined number of interpretable rules (P) and is based on the reasoning that if isolation of the rules promotes interpretability of the system, its approximation capacities depend heavily on the level of rule interpolation that takes place within the system. Therefore, initially we have an interpretable model with high rule isolation level and by gradually increasing interpolation zones in appropriate manner we should ultimately reach a satisfying result. Initialization, consequent and antecedent parameter identification and completion of the optimization algorithm are described in the following sections.

5.1 Input partition initialization

Unless we have a better idea, initialization of input MF parameters is based on H cluster centers $[x_{1h}, x_{2h}, \dots, x_{Nh}, y_h]$ extracted from training data by Gustafson-Kessel clustering algorithm (¹²). Given a preset interpolation/isolation ratio $\eta = [0, 1]$, input

partition of the primary model (Fig. 11) is initialized as follows

$$(i = 1, \dots, N, h = 1, \dots, H - 1)$$

$$c_i^h = a_i^{h+1} = x_i^h + \frac{(x_i^{h+1} - x_i^h)}{2}(1 - \eta) \quad (18)$$

$$d_i^h = b_i^{h+1} = c_i^h + (x_i^{h+1} - x_i^h)\eta \quad (19)$$

$$a_i^1 = b_i^1 = x_i^{\min}, c_i^H = d_i^H = x_i^{\max}$$

Note that $\forall i = 1, \dots, N, (S_i = H)$.

Figure 11

Input partition of the secondary model is constructed from the primary one according to (12) and (13).

5.2 Consequent Parameter Identification

To obtain consequent parameters for the two models, the following two-step procedure is used: in first pass consequent parameters of both models are identified together by using (5), with $\Gamma = [\Gamma_1, \Gamma_2]$, $\Gamma_1 = [W_1 X_e, \dots, W_p X_e, \dots, W_P X_e]$, $\Gamma_2 = [W_1 X_e, \dots, W_q X_e, \dots, W_Q X_e]$, $\theta = [\theta_1, \theta_2]$, $\theta_1 = [p_1, \dots, p_p, \dots, p_Q]^T$, $\theta_2 = [p_1, \dots, p_q, \dots, p_Q]^T$,

At this point, regardless of the actual configuration of the secondary model, we are making the assumption that it is a 1st order TS system just as the primary one.

In the second pass, however, consequent parameters of the secondary model will be properly re-identified, using

$$\theta_2 = [\Gamma_2^T \Gamma_2]^{-1} \Gamma_2^T (y - \Gamma_1 \theta_1) \quad (20)$$

Note that the formation of Γ_2 and what is contained in θ_2 depends on the order of consequent function and in case of 0th order function

$$x_k = [], p_q = p_0 q. \quad (21)$$

In case of 2nd order function (16)

$$\mathbf{x}_k = [x_1(k), (x_1(k))^2, x_2(k), (x_2(k))^2, \dots, x_N(k), (x_N(k))^2] \quad (22)$$

$$\mathbf{p}_q = [p_{0q}, p_{1q}^{(1)}, p_{1q}^{(2)}, \dots, p_{iq}^{(1)}, p_{iq}^{(2)}, \dots, p_{Nq}^{(1)}, p_{Nq}^{(2)}]$$

and in case of 3rd order function (17)

$$\mathbf{x}_k = [x_1(k), (x_1(k))^2, (x_1(k))^3, \dots, x_N(k), (x_N(k))^2, (x_N(k))^3] \quad (23)$$

$$\mathbf{p}_q = [p_{0q}, p_{1q}^{(1)}, p_{1q}^{(2)}, p_{1q}^{(3)}, \dots, p_{iq}^{(1)}, p_{iq}^{(2)}, p_{iq}^{(3)}, \dots, p_{Nq}^{(1)}, p_{Nq}^{(2)}, p_{Nq}^{(3)}]$$

5.3 Input partition optimization

After the model is initialized and consequent parameters are identified, we proceed with iterative input partition optimization. In each step of the cycle, k^{th} training sample (of all K samples) responsible for the maximum error $\varepsilon(k)$ is identified. Each i^{th} component of this sample will then be projected onto respective axis of x_i and fired MFs ($\mu_i^s(x_i(k)) > 0, \gamma_i^t(x_i(k)) > 0$) of both models will be updated according to the following rules. There are three possibilities (Figs. 12-13).

a) $x_i(k)$ falls into the isolated zone of the primary model (i.e. only μ_i^s has nonzero firing degree);

b) $x_i(k)$ falls into the left side of interpolation zone (i.e. μ_i^s and μ_i^{s+1} have both nonzero firing degrees and $\mu_i^s(x_i(k)) > \mu_i^{s+1}(x_i(k))$);

c) $x_i(k)$ falls into the right side of interpolation zone (i.e. μ_i^{s-1} and μ_i^s have both nonzero firing degrees and $\mu_i^s(x_i(k)) > \mu_i^{s-1}(x_i(k))$).

In case (a), the core ($c_i^s - b_i^s$) of μ_i^s (Fig. 10) is reduced from both sides by a preset value of Δx . Note that in order to satisfy conditions (12), some parameters of neighboring MFs also need to be updated.

In case (b), the core of μ_i^s is reduced from the right side and μ_i^{s+1} has to be updated

as well.

In case (c), the core of μ_i^s is reduced from the left side and d_i^{s-1} has to be updated as well.

Figure 12

Figure 13

Obviously, respective input MFs of the secondary model also need to be updated on the basis of (13). To complete the training step, it is followed by consecutive application of (5) and (20). Optimization is finished if the stopping criterion (which may be a preset number of training epochs, preset error value or preset error change rate) becomes satisfied.

6. Results

This section presents three examples² of function approximation to demonstrate how the proposed model configuration and the optimization algorithm deal with accuracy-transparency tradeoff. The first example is a function (24) from ⁽¹³⁾

$$y = 0.6 \sin(\pi x) + 0.3 \sin(3\pi x) + 0.1 \sin(5\pi x), \quad (24)$$

approximated from 201 data points placed at equal intervals in $[-1, 1]$ of input space.

We model this function using models with 3, 5 and 9 rules and using different types (constant, 1st order, (9) and (10)) of consequent functions. The results, evaluated with modeling root mean square error (RMSE) and final interpolation/isolation rate

$$\eta_{final} = 1 - \frac{1}{x_i^{\max} - x_i^{\min}} \sum_{s=1}^{S_i} b_i^s - c_i^s, \quad (25)$$

are given in Table 2, where L denotes the number of training steps necessary to obtain

² Note that the application of the proposed method for the approximation of (10) in section 2 with $\eta = 0.1$ and $\Delta x = 0.1$ in 16 training steps results in a model with RMSE = 0.0097 and $\varepsilon_i = 0.0311$ (see Table 1 for comparison).

minimum value of RMSE. Note that $\eta = 0.5$ and $\Delta x = 0.02$ in all experiments.

Table 2

The question here, as it turns out, is not so much how to obtain small RMSE (as it appears, the error falls into the same range, independent of P , except for some experiments with 0th order consequent functions in the secondary model) but how much interpretability we need to sacrifice (expressed by η_{final}). In present case, 2nd order consequent function seems to be the optimal choice. One must take into account, however, that computation of higher order function parameters requires more computational power and increases model complexity. Increase of P similarly pays back with more interpretability (Fig. 14) and faster convergence but must be weighted against system complexity.

Figure 14

In the second example the algorithm has to deal with noisy/corrupt motorcycle crash data taken from (¹⁴). The iterative approach is not appropriate here because a single strongly biased outlier can outbalance it. Therefore the procedure is skipped and the input partition obtained by initialization serves as the final partition. Secondly, to ensure smooth interpolation (because of noise secondary model may obtain non-smooth interpolating local models), linear coefficients p_{iq} of the 1st order secondary model are computed as the average of respective coefficients from the relevant (active in the same region) rules of the primary model so that

$$p_{iq} = \underset{\tau_p(c_q) > 0}{\text{avg}} (p_{ip}), \quad (26)$$

where $c_q = [(\beta_{1r} + \chi_{1r})/2, \dots, (\beta_{Nr} + \chi_{Nr})/2]$ is the center of q^{th} rule in input space. The remaining unknown parameters of the secondary model (p_{0q}) are identified using least squares estimator, so that

$$[p_{01}, \dots, p_{0Q}]^T = [\Gamma_2^T \Gamma_2]^{-1} \Gamma_2^T (y - \Gamma_1 \theta_1 - \Gamma_2 \varphi), \quad (27)$$

where $\varphi = [p_{11}, \dots, p_{N1}, \dots, p_{1q}, \dots, p_{iq}, \dots, p_{Nq}, \dots, p_{1Q}, \dots, p_{NQ}]^T$ contains the coefficients computed by (21).

Figure 15

Using the settings $P = 4$, $Q = 3$, $\eta = 0.5$ and applying (21-22) we see from Fig. 15 that four extracted interpretable local models capture the essence of the process under consideration. Moreover, in comparison with the results obtained in ⁽⁵⁾ with different combinations of global and local least squares, our result (MSE = 467.68) is outperformed only by a pure global least-squares approach (MSE = 460.62) with very poor interpretability, even then, in our experiment overall 7 rules are used, compared to 8 in ⁽⁵⁾.

Finally, an approximation of 3D function

$$y = (x_1 - 1)^5 + (x_2 - 1)^5 \quad (28)$$

is presented, using 441 data points spaced equidistantly in $[-1, 1] \times [-1, 1]$ of input space.

Figure 16

After 30 steps of training ($P = 4$, $Q = 5$, $\eta = 0.02$, $\Delta x = 0.02$) using (9) in the secondary model, we obtain RMSE = 0.5596 (Fig. 16), which is about 2.5 times less than the number (1.3927) obtained in ⁽¹¹⁾ (important note: the result in ⁽¹¹⁾ is obtained with just four rules). The current approach, however, is more universal, as it does not assume anything about the type of rule interpolation unlike the method described in ⁽¹¹⁾.

7. Conclusions

We have introduced a two-model system configuration to improve both interpretability and interpolation in TS modeling and developed the optimization method to fully exploit the properties of the proposed configuration. The experiments show that the proposed approach is able to extract legitimate TS local models from data. Evaluation of models in terms of modeling RMSE and rule interpolation/isolation ratio also indicates that final result depends on the initialization procedure of the model (the number of fuzzy rules and initial model parameter values). Special measures to deal with noisy data are suggested. These results provide the platform for fuzzy gain-scheduling control what will be our immediate research topic.

References

1. T. Takagi, M. Sugeno, "Fuzzy identification of systems and its applications to modeling and control," IEEE Trans. Syst., Man, Cybernetics, SMC-15-1, 116-132, (1985).
2. P. Viljamaa, "Fuzzy Gain Scheduling and Tuning of Multivariable Fuzzy Control - Methods of Fuzzy Computing in Control Systems," Ph.D. dissertation, Automation and Control Institute, Tampere Univ. of Technology, (2002).
3. J. Casillas, O. Cordon, F. Herrera, L. Magdalena, Ed. "Interpretability Issues in Fuzzy Modeling," Springer, (2003).
4. J. Abonyi, "Fuzzy Model Identification for Control," Birkhäuser, (2003).

5. J. Yen, L. Wang, C.W. Gillespie, "Improving the Interpretability of TSK Fuzzy Models by Combining Global Learning and Local Learning," *IEEE Trans. Fuzzy Systems*, 6-4, 530-537, (1998).
6. A. Riid, "Transparent Fuzzy Systems: Modeling and Control," Ph.D. dissertation, TTU Press (2002).
7. S. L. Chiu. "A Cluster Estimation Method with Extension to Fuzzy Model Identification," *Proc. IEEE Int. Conf. on Fuzzy Systems*, 1240-1245, (1994).
8. M. Setnes, R. Babuska, H.B. Verbruggen, "Rule-based modeling: precision and transparency", *IEEE Trans. Systems, Man, and Cybern. - Part C*, 29 (1), 165-169, (1999).
9. W.S. Cleveland, "Robust locally weighted regression and smoothing scatterplots," *J. Amer. Statistical Assoc.*, 74, 829-836, (1979).
10. A Riid, R. Isotamm, E. Rüstern "Transparency Enhancement of 1st order TS systems: Promoting the Competition Between the Rules by Controlling the Overlap of Input Fuzzy Sets," *Proc. 8th Biennial Baltic Electronic Conf.*, 137-140, (2002).
11. R. Babuska, C. Fantuzzi, U. Kaymak, H.B. Verbruggen, "Improved inference for Takagi-Sugeno models," *Proc. IEEE Int. Conf. Fuzzy Syst.*, 701-706, (1996).
12. D.E. Gustafson, W.C. Kessel, Fuzzy clustering with a fuzzy covariance matrix." *Proc. IEEE Conf. Decision and Control*, 761-766, (1979).
13. J.-S. R. Jang, "ANFIS: Adaptive-network-based fuzzy inference system," *IEEE Trans. System, Man, Cybernetics*, 23-3, 665-685, (1993).
14. W.Hardle, "Applied Nonparametric Regression," Cambridge Univ. Press, (1990).

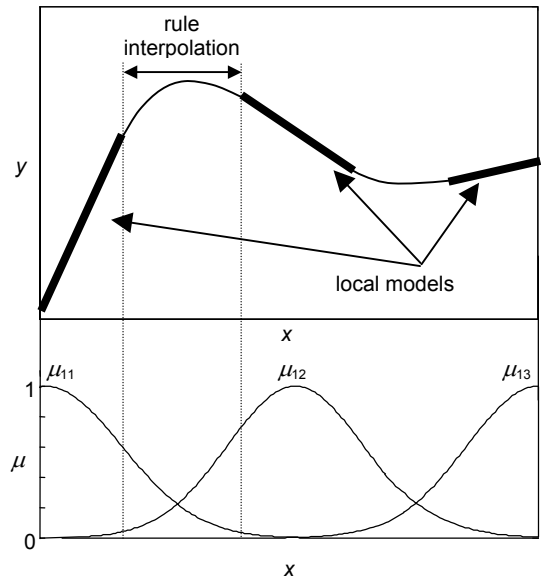


Fig. 1. Idealistic view of 1st order TS systems

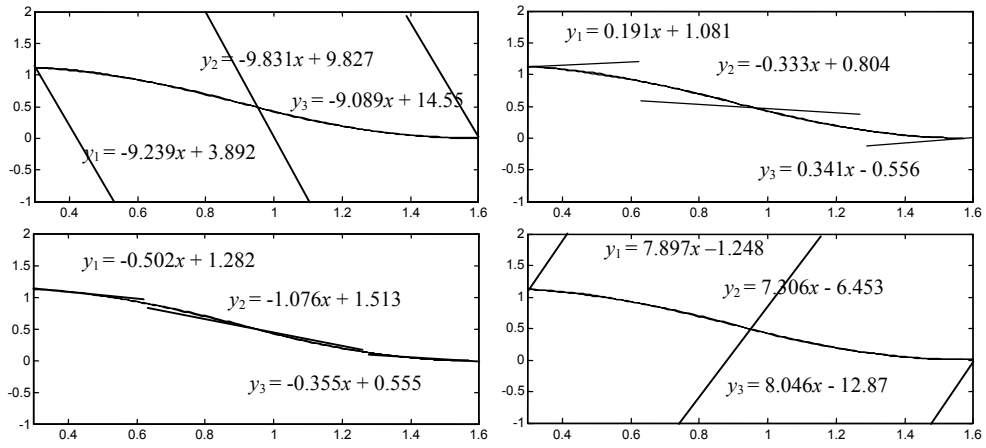


Fig. 2. Non-identifiability in 1st order TS systems

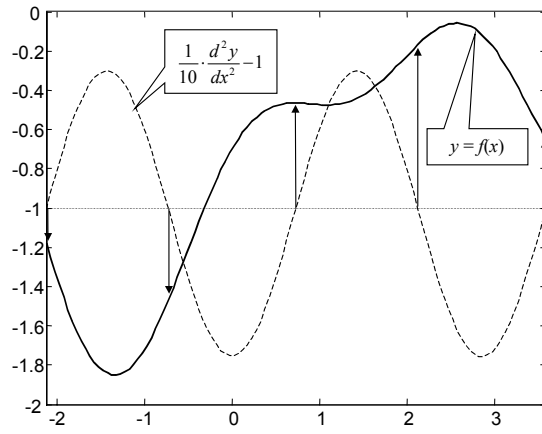


Fig. 3. Function (10) and centers of input MFs

Method	RMSE	ε_l
Global	0.0105	0.1189
Global-local	0.0240	0.0692
Exponential	0.0223	0.0761

Table 1. Modeling results of (10).

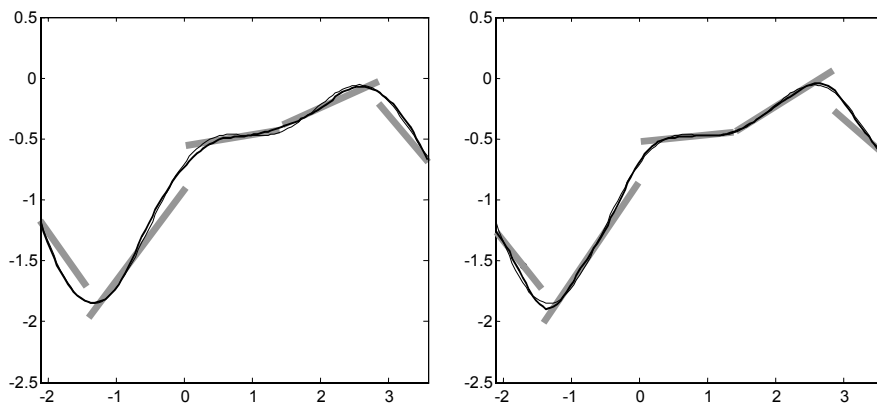


Fig. 4. Approximation of (10) by global-local least squares (left) and rule exponents (right).

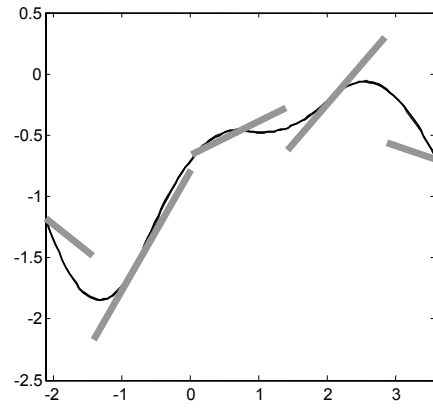


Fig. 5. Approximation of (10) by global least squares

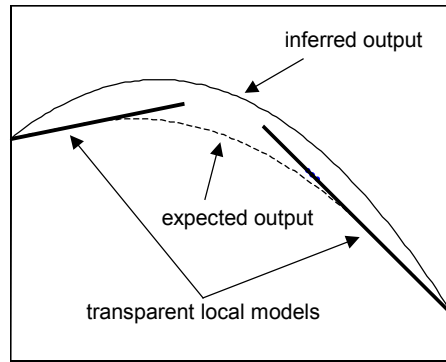


Fig. 6. Biased global output from interpretable local models.

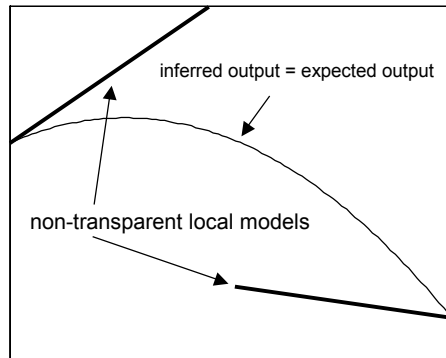


Fig. 7. Biased local models to produce acceptable global output

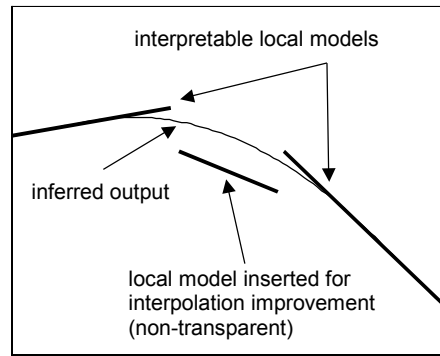


Fig. 8. Interpolation improvement by rule insertion

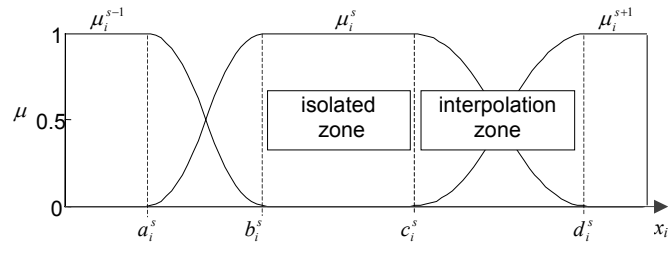


Fig. 9. Input partition of the primary model.

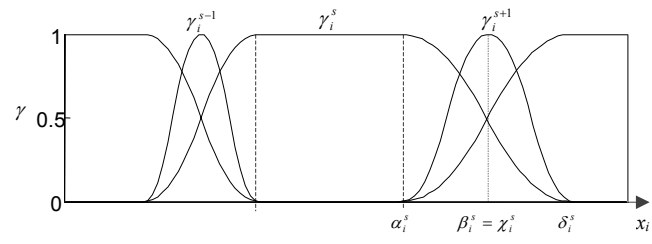


Fig. 10. Input partition of the secondary model

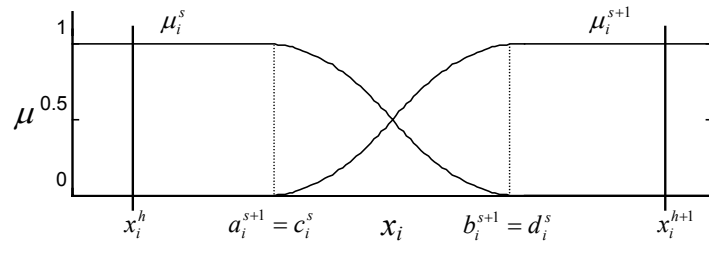


Fig. 11. Extraction of MFs of the primary model from cluster centers.

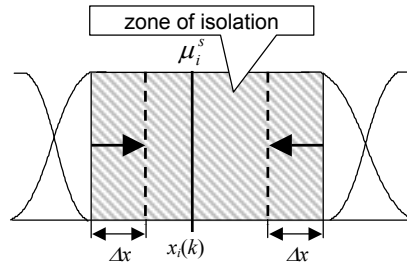


Fig. 12. Modification of MFs if $x_i(k)$ falls into isolated zone.

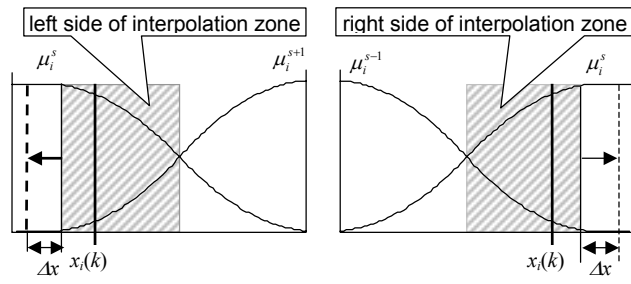


Fig. 13. Modification of MFs if $x_i(k)$ falls into interpolation zone.

$P(Q)$	rank of y_q	RMSE	η_{final}	L
3 (5)	0 / 1	0.0071/0.0071	0.9679/0.9679	66/62
3 (5)	2 / 3	0.0071/0.0085	0.9679/0.9579	61/60
5 (9)	0 / 1	0.0143/0.0087	0.6000/0.6900	16/21
5 (9)	2 / 3	0.0064/0.0063	0.6900/0.6900	21/21
9 (17)	0 / 1	0.1180/0.0059	0.5100/0.5900	7/15
9 (17)	2 / 3	0.0045/0.0044	0.5900/0.5900	13/13

Table 2. Modeling results of (24).

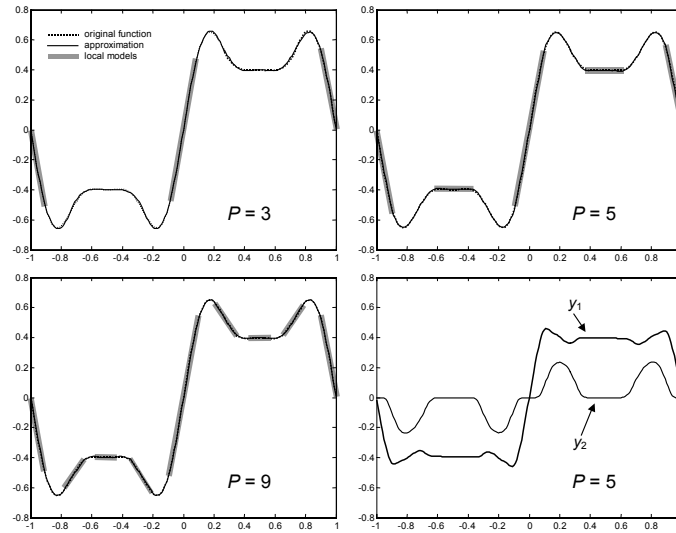


Fig. 14. Approximation of (24). Lower right figure depicts the outputs of both models, respectively.

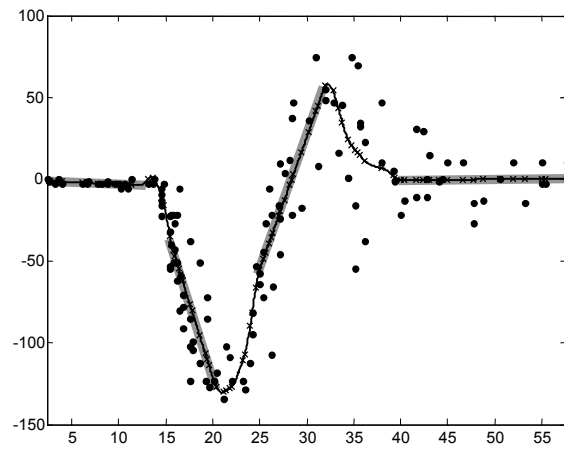


Fig. 15. Approximation of motorcycle data. Legitimate local linear models are depicted with gray lines.

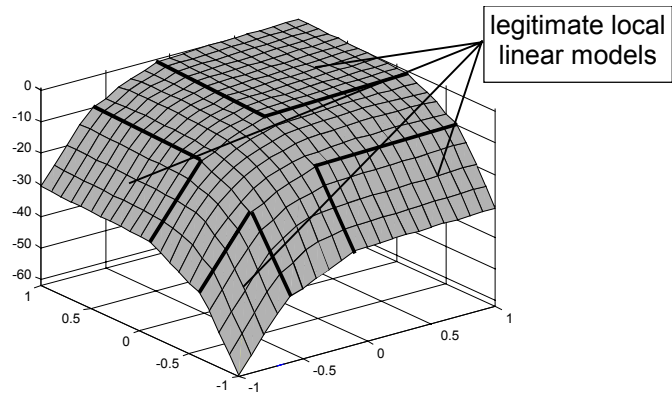


Fig. 16. Approximation of 3D data.